Raman Scattering and Photoluminescence in Boron-Doped and Arsenic-Doped Silicon

J. M. Cherlow,*† R. L. Aggarwal, and B. Lax*

Francis Bitter National Magnet Laboratory,‡ Massachusetts Institute of Technology, Cambridge, Massachusetts 02139

(Received 1 February 1973)

The deformation potentials and g values of the ground state of the boron acceptor in silicon have been determined from a study of the stress and Zeeman splitting of the electronic Raman scattering in this material. The stress splitting of the Raman line results from a twofold splitting of the Γ_8 ground state only and yields the shear deformation potentials $b' = -1.46 \pm 0.06$ eV and $d' = -4.16 \pm 0.12$ eV. The temperature dependence of the Zeeman spectra indicates that the observed Zeeman components arise only from a splitting of the acceptor ground state. This conclusion is supported by the anisotropy of the Zeeman pattern which is characteristic of the splitting of a Γ_8 level. An analysis of the Zeeman splittings yields the phenomenological average g value squared $M^2 = 1.23 \pm 0.04$ and the anisotropy parameter $\epsilon = -0.07 \pm 0.02$. The corresponding parameters of the Luttinger spin Hamiltonian are $K = 0.84 \pm 0.09$ and $L = 0.13 \pm 0.08$ in contrast to the values of $K = 1.21 \pm 0.01$ and $L = 0.00 \pm 0.01$ obtained by Feher, Hensel, and Gere using paramagnetic resonance in uniaxially stressed samples. The g values obtained from magneto-Raman measurements on stressed samples are consistent with the zero-stress magneto-Raman results, and the discrepancy between the two sets of experimental results remains unexplained. The Zeeman splitting of the photoluminescence of excitons bound to neutral arsenic donors has been interpreted in terms of a simplified model of the silicon band structure. For the g value of the hole in the bound-exciton complex we obtain $M^2 = 1.44 \pm 0.07$ and $\epsilon = -0.12 \pm 0.04$ corresponding to $K = 0.74$ and $L = 0.22$; for the g value of the ground state of the arsenic donor we get $g_e = 1.85 \pm 0.06$. The electronic g value is in disagreement with electron-spin-resonance results. A quadratic diamagnetic shift of the bound exciton is also observed.

I. INTRODUCTION

Optical experiments have been used extensively to study the properties of impurities in silicon. In particular, infrared absorption[1,2] and electronic Raman scattering[3-5] experiments have yielded a great deal of information regarding the nature of the electronic states of neutral impurity atoms in silicon. In an electronic Raman transition in a semiconductor an electron or a hole is raised from the impurity ground state to an excited state. Because the Raman process is a two-photon process, the selection rules are, in general, complementary to those for infrared absorption. Photoluminescence experiments[6-9] have been used to investigate the properties of excitons bound to impurities in silicon as well as those of impurity states. The common aspect in these two types of experiments is the study of the properties of electrons or holes bound to impurity atoms.

In boron-doped silicon Wright and Mooradian observed a single electronic Raman line[3] which splits into two components with the application of uniaxial stress.[5] This line corresponds to an electronic (hole) transition from the fourfold degenerate Γ_8 acceptor ground state[2] to an excited acceptor state whose effective-mass envelope function has positive parity. The energy of the Raman-active excited state, measured from the ground state, is less than that of any of the infrared-active excited states. The uniaxial stress result is

consistent with the existence of a ground-state splitting only, and indicates that the excited state is a Kramers doublet. Similar experiments have been performed in gallium phosphide by Henry et al.[10] and by Manchon and Dean,[11] who have discussed the nature of the excited state in terms of Jahn–Teller coupling.[12]

In this paper we report a detailed study of the stress splittings and Zeeman splittings of the Raman line. From these measurements we have calculated the deformation potentials and g values of the acceptor ground state; previous infrared magnetospectroscopic measurements[13] have not yielded numerical values for the g factor. The g values have been measured, however, in a paramagnetic resonance experiment.[14] A comparison of the two sets of results will be presented. A brief account of a part of this work has been given previously.[15,16]

Photoluminescence from bound excitons in silicon was first observed by Haynes[6] following a suggestion by Lampert[17] and later studied in more detail by Dean et al.[7] Here we report a study of the Zeeman splitting of the photoluminescence of excitons bound to arsenic donors in silicon.[18] These results are analyzed in terms of the model developed by Thomas et al.[19,20] for bound excitons in gallium phosphide and yield g values for the bound-exciton complex and for the ground state of the arsenic donor. The results for the ground state of the donor are compared with those of microwave resonance experiments.[21]

II. THEORY

A. Acceptor States

A description of acceptor impurity states in silicon is complicated by the complex nature of the valence band in silicon. At the center of the Brillouin zone the $p_{3/2}$ valence-band edge is four-fold degenerate and has Γ_8^+ symmetry; the two-fold degenerate $p_{1/2}$ spin-orbit split-off band has Γ_7^+ symmetry and lies 44 meV below the valence-band edge.[22] Because the spin-orbit splitting Δ is of the same order as the observed ionization energies for acceptors in silicon, all six of the valence bands in silicon must be considered in a calculation of the energy levels for the acceptor impurity.

In the effective-mass approximation the total wave function of an acceptor state can be written as the sum of products of the envelope functions satisfying the effective-mass equation and the band-edge Bloch functions.[23] The sum is over all the valence bands. Using a variational technique Schechter[24] has solved the effective-mass equation and has calculated the energies of the acceptor ground state and the excited states with $2p$ envelope functions associated with the $p_{3/2}$ valence-band edge. A more detailed variational calculation using six component wave functions for the ground-state energy has been carried out by Suzuki et al.[25] The calculation indicates that the ground state is primarily s like but also that a small d-like part plays a significant role in determining the energy.

External static fields such as magnetic and strain fields can lower the tetrahedral symmetry of the acceptor impurity atoms and thereby split the four-fold degenerate ground state. The first-order effect of the shear components of an external stress is a splitting of the quartet into two Kramers doublets. The splitting can be described by the spin Hamiltonian

$$\mathcal{H}_{st} = - b' \left[(J_x^2 - \tfrac{1}{3} J^2) e_{xx} + (J_y^2 - \tfrac{1}{3} J^2) e_{yy} + (J_z^2 - \tfrac{1}{3} J^2) e_{zz} \right] - \tfrac{1}{3} \sqrt{3} \, d' \left(\{ J_x J_y \} e_{xy} + \{ J_y J_z \} e_{yz} + \{ J_z J_x \} e_{zx} \right) . \quad (1)$$

Equation (1) can be regarded as the projection onto $J = \frac{3}{2}$ space of the shear part of the orbital strain Hamiltonian[26] for the valence-band edge. The deformation potentials b' and d' are analogous to those introduced by Pikus and Bir[26] for the valence-band edge and are proportional to those of Kleiner and Roth.[27] By carrying out the projection according to the procedure described by Luttinger[28] and using their effective-mass wave functions, Suzuki et al.[25] have calculated the ratios of the acceptor ground-state deformation potentials to the valence-band-edge deformation potentials. They obtained

$$b'/b = 0.775, \quad d'/d = 0.971 . \quad (2)$$

This result should hold only in the low-stress regime where the stress-induced mixing of the $m_J = \pm \frac{1}{2}$ valence band with the split-off band can be ignored.[29] The positive ratios in Eqs. (2) are consistent with the experimental results that the $m_J = \pm \frac{1}{2}$ eigenstates are lower in hole energy for both the acceptor ground state[14] and for the valence-band edge.[30] As is the case for the valence-band edge, the magnetic quantum number remains a good quantum number only for stress along $\langle 100 \rangle$ and $\langle 111 \rangle$ axes.

The spin Hamiltonian for a Γ_8 state, such as the acceptor ground state, was given by Bleaney[31] and by Luttinger[28] as

$$\mathcal{H}_{Zee} = \mu_B \left[K \vec{J} \cdot \vec{H} + L (J_x^3 H_x + J_y^3 H_y + J_z^3 H_z) \right] . \quad (3)$$

Very recently the case of a spin Hamiltonian including terms quadratic in the magnetic field has been treated by Bhattacharjee and Rodriguez[32] in a theoretical study of the Zeeman splitting of acceptor levels. Suzuki et al.[25] have calculated values for the phenomenological parameters K and L in Eq. (3). In their calculation they considered three types of interaction of the external magnetic field with the hole: (i) the interaction with the orbital angular momentum, (ii) the interaction with the spin, and (iii) the interaction with the nonperiodic part of the orbital angular momentum. The third interaction arises from the substitution $\vec{p} \rightarrow \vec{p} - e\vec{A}/c$ in the effective-mass Hamiltonian. Their calculation yielded the results

$$g_{1/2} = 0.97, \quad 3g_{3/2} = 3.66, \quad K = 0.93, \quad L = 0.13. \quad (4)$$

Here $g_{1/2}$ and $g_{3/2}$ are the g factors for $\vec{H} \parallel [001]$. The existence of a nonzero cubic term L in Eq. (3) is equivalent to the nonuniform spacing of the Zeeman-split levels. It arises from the lack of spherical symmetry of the ground-state wave function which is a result of the warped nature of the valence bands. That L can be nonvanishing even though Luttinger's constant q is negligible was first pointed out by Yafet and Thomas.[20]

The calculated results (2) and (4) have the same inherent limitations as all effective-mass calculations. In addition, they are very sensitive to the numerical values of the band-edge parameters; the values used by Suzuki et al.[25] are not the most recent ones.[33] A similar calculation has been performed by Bir et al.[34] Their results for the deformation potentials are in good agreement with those of Suzuki et al.[25] However, their results for the g values differ greatly because they ignored the third contribution to the Zeeman Hamiltonian given above.

To calculate the g value of the ground state for

an arbitrary direction of the magnetic field, the spin Hamiltonian of Eq. (3) must be solved for this field direction. Bleaney[31] first obtained a general solution of Eq. (3); his results have been reexpressed by Yafet and Thomas[20] as

$$9g_0^2 = M^2 \{ 5 + 4[1 + 15(1 + \epsilon)$$
$$\times (l^2 m^2 + m^2 n^2 + n^2 l^2 - \tfrac{1}{5}) - \epsilon^2]^{1/2} \} , \quad (5)$$

and

$$g_i^2 = M^2 \{ 5 - 4[1 + 15(1 + \epsilon)$$
$$\times (l^2 m^2 + m^2 n^2 + n^2 l^2 - \tfrac{1}{5}) - \epsilon^2]^{1/2} \} . \quad (6)$$

Here g_0 and g_i are the observed g values with $\tfrac{3}{2} g_0 \geq \tfrac{1}{2} g_i \geq 0$, and l, m, n are the direction cosines of the applied magnetic field with respect to the crystal axes. Equations (5) and (6) relate the observed g values to the phenomenological parameters M^2 and ϵ. M^2 is an "average" g value squared and can be expressed as

$$10 M^2 = 9 g_0^2 + g_i^2 , \quad (7)$$

while ϵ characterizes the deviation from spherical symmetry and can be written

$$M^2 (1 + \tfrac{8}{3} \epsilon) = g_0(\langle 001 \rangle) g_i(\langle 001 \rangle) . \quad (8)$$

The experimentally measured Zeeman splitting of a Γ_8 level determines M^2 and ϵ uniquely, but for a given M^2 and ϵ there is an eightfold ambiguity in the values of K and L; that is, the magnetic sublevels can be ordered in eight different ways. The calculations of Suzuki et al.[25] indicate that in the case of the acceptor ground state, they are ordered $\tfrac{3}{2}$, $\tfrac{1}{2}$, $-\tfrac{1}{2}$, $-\tfrac{3}{2}$. This is the same ordering as was observed by Yafet and Thomas[20] for bound excitons in GaP and their equations

$$M^2 = K^2 + \tfrac{41}{10} KL + \tfrac{73}{16} L^2 \quad (9)$$

and

$$\epsilon = - (\tfrac{3}{5} KL + \tfrac{3}{2} L^2)/M^2 , \quad (10)$$

apply here; this ordering is the one that occurs for $L = 0$.

Morgan[12] has considered the effects of the coupling of the acceptor ground state to local distortion of the lattice through the dynamic Jahn–Teller effect. He points out that, because of the orbital degeneracy of the Γ_8 valence band, each of the four components of a purely electronic hole state is mixed with other components by phonons with E and T_2 symmetry. The resulting vibronic state has the same symmetry as the unmixed state but exhibits different electronic properties. He has shown that the anisotropic g value is increased by the vibronic coupling and that the deformation potentials are decreased. Morgan[35] has also considered the effect of local electrostatic and strain fields surrounding misfitting substitutional im-

purities on the ground state.

Phillips[36] has analyzed the chemical shifts of the ground-state energies and g factors of various acceptors in silicon based on his spectroscopic theory of the covalent bond. His result is isotropic.

The existence of a Raman-active excited state was not predicted by the effective-mass calculations which considered only infrared-active excited states. Wright and Mooradian[5] have proposed that the Raman active state is formed from a product of a $1s$ envelope function with a $p_{1/2}$ band-edge function. That such a state should exist so close to the acceptor ground state is surprising; Manchon and Dean[11] have speculated as to how static or dynamic Jahn–Teller coupling could account for the existence of such a state in the position in which it is observed in gallium phosphide.

B. Bound Excitons

Excitons bound to neutral impurities are immobile four-particle complexes consisting of, for example, two electrons, a hole, and a positive donor ion (or, on the other hand, two holes, an electron, and a negative acceptor ion). Hopfield[37] has shown by considerations of simple quantum chemistry that these complexes should be stable in all semiconductors.

The model developed by Thomas et al.[19,20] to explain the Zeeman splitting of photoluminescence from excitons bound to neutral donors in gallium phosphide can be used to explain the analogous phenomenon in silicon. Thomas et al. have argued that the low temperature optical properties of excitons bound to neutral donors in an indirect gap material show no explicit effects arising from the multivalley nature of the conduction band. In this model both of the electrons in the bound exciton-complex have orbital singlet wave functions. Thus their spins are antiparallel, and they do not contribute to the g value of the bound exciton. The bound-exciton complex then has the g values of the Γ_8 hole. The appropriate spin Hamiltonian is then that given in Eq. (3), which we discussed above. The formalism for the two cases is the same because in both cases we are considering bound holes with Γ_8 symmetry. For the dominant radiative decay process the final state of the transition is a neutral donor with an electron in the ground state. This electron has an isotropic g value,[38] so any anisotropy in the Zeeman spectrum can be attributed to the hole.

Figure 1, taken from Thomas et al.,[19] illustrates the possible Zeeman components; the intensities and polarizations are calculated from the simple selection rules of atomic physics. The model predicts six allowed Zeeman components, four with electric vector polarized perpendicular to the magnetic field and two with electric
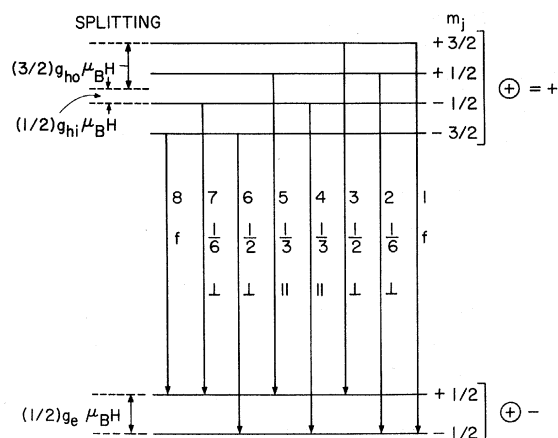
SPLITTING

FIG. 1. Schematic diagram of "simplified" model for Zeeman splitting of photoluminescence from excitons bound to neutral donors showing polarization and relative amplitudes for each of the allowed components. (The forbidden components are denoted by f.)

vector parallel to the magnetic field.

III. EXPERIMENTAL

A pulsed Nd^{3+} : YAG laser operating at a wavelength of 1.064 μm was used to excite Raman scattering from liquid helium cooled, oriented, single crystal specimens of silicon. The energy output of the laser was of the order of 0.1 J per pulse, and the duration of each pulse was about 100 μsec. Sample heating considerations limited the pulse repetition rate to 1–2 pulses per second. The photon energy of the laser, 1.164 eV, is just slightly less than the absorption threshold of pure silicon at low temperatures. [39] Hence the use of this laser allows a large volume of the crystal to be utilized for Raman scattering.

The silicon samples used were cut from single crystal ingots and were oriented by the Laue back reflection method. The samples were lapped and etched in order to produce shiny surfaces. The samples used for the Raman experiments were doped with ~ 5×10^{15} cm^{-3} atoms of boron.

The samples were cryogenically cooled either by being immersed in liquid helium, by being mounted on a cold finger in contact with a helium reservoir, or by being mounted in a cold-finger stress rig. This compressional stress rig was similar to that described by Pollak and Cardona. [40] Magnetic fields up to about 92 kG were applied to the samples by means of a water-cooled Bitter solenoid which has radial access in two dimensions and a $2\frac{1}{8}$-in. bore. Radiation scattered at 90° was analyzed by a Spex Model 1400 double monochromator and detected by a cooled EMI 9684 photomultiplier tube with $S1$ response. The output of the photomultiplier tube was averaged by a boxcar

integrator and displayed on a strip-chart recorder. The data were later digitized from the recorder tracings and replotted to facilitate the comparison of experimental and calculated results.

No direct measurements of the sample temperature were possible because the temperature inside the sample is expected to be different from that at the surface as a result of a small amount of absorption of the laser radiation.

The experimental system described above was also used to study the Zeeman splitting of bound-exciton photoluminescence. Although the photon energy of the laser was below the intrinsic absorption threshold of silicon the small amount of impurity induced absorption was sufficient to create photoluminescence. Laser excitation in this study and in that of Pokrovskii et al. [41] made possible a much higher resolution than that obtained in the early photoluminescence experiments using mercury lamp excitation. The silicon samples used for the photoluminescence experiment were doped with ~ 1×10^{16} cm^{-3} atoms of arsenic.

IV. RESULTS AND DISCUSSION

A. Acceptor Ground-State Deformation Potential Measurements

Figure 2 shows the electronic impurity Raman line in boron-doped silicon as a function of uniaxial stress along a $\langle 111 \rangle$ direction. At low stresses this line clearly splits into two compo-
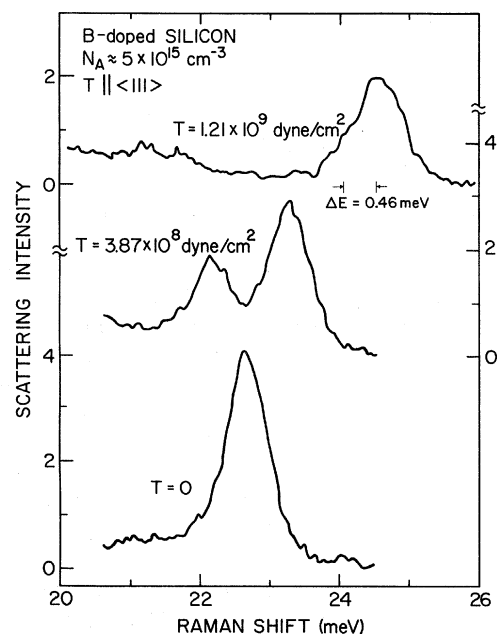
FIG. 2. Stress splitting of electronic (hole) Raman scattering in boron-doped silicon.

nents. At the higher stresses the low-energy component almost completely disappears. This behavior is what is expected from the thermalization of a ground-state splitting. It confirms the interpretation of Wright and Mooradian[5] who identified this stress splitting of the Raman line as resulting only from a stress splitting of the acceptor ground state. It should be pointed out that the high energy Raman component is a result of a transition from the Kramers doublet with the lower hole energy. The zero-stress position of the Raman line which we measured as 22.7 meV differs slightly from Wright and Mooradian's measurements of 23.4 meV.

The stress split components are somewhat wider than the zero-stress line. We attribute the broadening to inhomogeneity in the stress; special care in sample preparation led to a reduced amount of line broadening. The line shapes in Fig. 2 are not the best that have been obtained.

We have studied the splitting of the Raman line as a function of stress for uniaxial stresses of up to about 3×10^9 dyn/cm^2 along $\langle 111 \rangle$ and $\langle 100 \rangle$ directions. The low-energy Raman component could be followed only up to a stress of about 8×10^8 dyn/cm^2. At higher stresses the intensity of this component was not sufficient for us to determine its position. In Figs. 3(a) and 3(b) the peak positions are shown as a function of stress applied along the $\langle 111 \rangle$ and $\langle 100 \rangle$ axes. In these figures the vertical error bars represent the estimated uncertainty in determining the position of the peaks. The random error in the determination of the stress is quite small, probably of the order of 10^7 dyn/cm^2. Systematic variation arising from stress inhomogeneity in the sample might be considerably greater.

The solid curves through the upper sets of experimental points are least-squares fits with a linear and a quadratic term. The dashed lines represent only the linear term in these fits. It is seen that the quadratic term contributes significantly. The solid lines through the data points for the low-energy component are linear fits to these points. There were not enough of these points for us to determine if there is any significant quadratic effect on this component. In the discussion which follows only a linear effect will be considered.

The linear deformation potentials are related to the observed splitting by

$$b' = \delta E(\langle 100 \rangle)/2 \, (S_{11} - S_{12}) \, T, \tag{11}$$

$$d' = \sqrt{3} \, \delta E(\langle 111 \rangle)/S_{44} T , \tag{12}$$

where $\delta E(\langle 100 \rangle)$ and $\delta E(\langle 111 \rangle)$ are the splittings given by the linear term used for the curves in Figs. 3(a) and 3(b), S_{11}, S_{12}, and S_{44} are the elastic compliance constants, and T is the applied com-
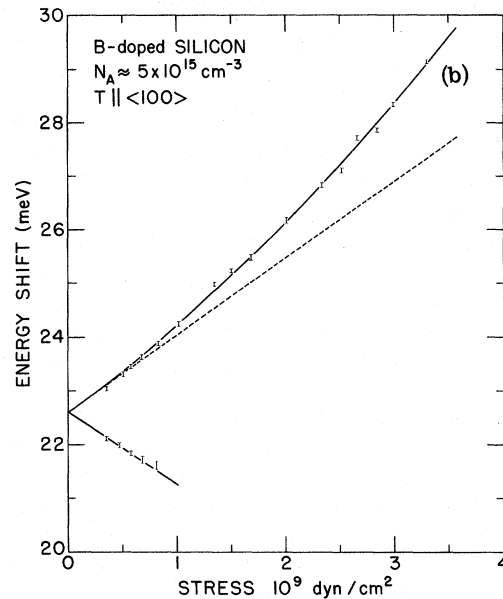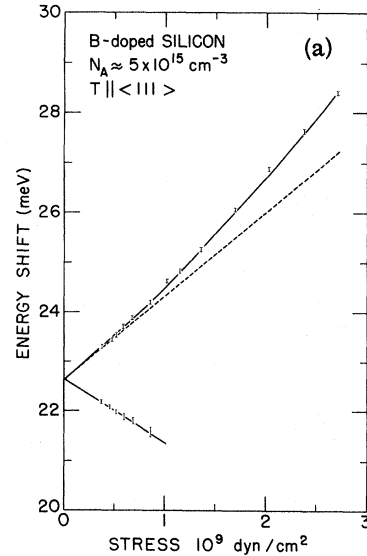
FIG. 3. Energy shift as a function of the applied stress for the two stress-split componenets of the electronic Raman scattering in boron-doped silicon: (a) stress T parallel to a $\langle 111 \rangle$ axis; (b) stress parallel to a $\langle 100 \rangle$ axis.

pressional stress. Using values of S_{11}, S_{12}, and S_{14} calculated from the elastic stiffness constants measured by Hall[42] for pure silicon at 4.2 °K we obtain

$$b' = - \, (1.46 \pm 0.06) \text{ eV} \tag{13}$$

and

$$d' = - \, (4.16 \pm 0.12) \text{ eV}. \tag{14}$$

The major contribution to the estimated errors in the deformation potentials is the error in the curve-

TABLE I. Deformation potentials of boron acceptor ground state and of valence-band edge in units of electron volts.

Band edge[a]	This work	Acceptor ground state Expt.[b]	Expt.[c]	Calc.[d]	Calc.[e]
$d = -(4.85 \pm 0.15)$	$d' = -(4.16 \pm 0.12)$	$-(4.50 \pm 0.15)$	$-(2.1 \pm 0.2)$	$-(4.70 \pm 0.15)$	$-(4.50 \pm 0.15)$
$b = -(2.15 \pm 0.10)$	$b' = -(1.46 \pm 0.06)$	$-(1.61 \pm 0.07)$	$-(0.66 \pm 0.04)$	$-(1.67 \pm 0.08)$	$-(1.80 \pm 0.06)$

[a]Laude et al., Ref. 45.   [c]Parsons, Ref. 44.   [e]Bir et al., Ref. 34.
[b]Chandrasekhar et al., Ref. 43.   [d]Suzuki et al., Ref. 25.

fitting procedure and a small contribution is due to the uncertainty in sample area. Systematic errors in the measurement of the applied stress cannot be estimated quantitatively.

In Table I we compare our results for the deformation potentials with other experimental measurements and with theoretical predictions. The experimental values of Chandrasekhar et al.,[43] and those of Parsons[44] were obtained from the stress dependence of the $2p'$ infrared absorption line[2] in boron-doped silicon. The measurements by Chandrasekhar et al.[43] were carried out under stresses of up to 9×10^8 dyn/cm^2. The theoretical values listed in the table were obtained from the ratios calculated by Suzuki et al.[25] [Eq. (2)] and similar ratios obtained by Bir et al.[34] and the optically measured band-edge deformation potentials of Laude et al.[45]

We note reasonable agreement between our experiment and that of Chandrasekhar et al.[43] However, the discrepancy between these two measurements on the one hand, and the unpublished measurement of Parsons[44] on the other hand, is quite serious and so far unexplained.

Our experimental results are in qualitative agreement with the theoretical predictions based on the effective-mass approximation. We have shown that the acceptor ground-state deformation potentials are slightly less than the band-edge values and also that the relative difference berween them is greater for the $\langle 100 \rangle$ deformation potentials than for the $\langle 111 \rangle$ deformation potential. Considering the inherent inadequacies of an effective-mass calculation this qualitative agreement is all that could be expected.

The negative signs of the deformation potentials are not explicitly determined by our experiment. However, this ordering of the stress-split sublevels of the impurity ground state has been firmly established by both microwave resonance[14] and infrared absorption experiments.[3,43]

For equal values of stress the energy differences between the lower component line and the dashed upper component line in Figs. 3(a) and 3(b) are equal within experimental error. That is, in the low-stress linear limit the splitting of the acceptor ground state is the same for equal amounts of stress in $\langle 100 \rangle$ and $\langle 111 \rangle$ directions. This result was also obtained by Chandrasekhar et al.,[43] and, as they have shown, implies an isotropic splitting of the acceptor ground state for a given compression.

The analysis of the quadratic shift of the high-energy component and of the linear shift of the center of gravity of the two components is less straightforward than the above. In the case of the linear deformation potential we were concerned only with the acceptor ground state while here we must consider the excited state as well as the ground state. The observed linear shift of the center of gravity is $(0.11 \pm 0.08) \times 10^{-9}$ meV cm^2/dyn for a $\langle 100 \rangle$ stress, and $(0.50 \pm 0.06) \times 10^{-9}$ meV cm^2/dyn for a $\langle 111 \rangle$ stress. A linear shift of the center of gravity might be expected as a result of the hydrostatic component of the strain; however, any hydrostatic contribution would be isotropic. No such linear anisotropic shift of the center of gravity was observed in the infrared absorption measurements.[43] Hence, it appears likely that this anisotropic shift is a property of the excited state and that the excited state couples more strongly to a $\langle 111 \rangle$ stress than to a $\langle 100 \rangle$ stress. This result gives some support to the hypothesis that the excited state is somehow coupled to the lattice by a vibronic interaction.

A quadratic shift of the high-energy component is expected because such a shift occurs for the stress split $M_j = \pm \frac{1}{2}$ valence-band edge as a result of stress-induced mixing with the split-off band. In the equations which give the energy of the $M_j = \pm \frac{1}{2}$ valence band (V_1 band) at $k = 0$ as a function of stress, the quadratic term can be written as a function of stress as

$$\frac{1}{2} \frac{(\delta E)^2}{\Delta} = \frac{1}{2\Delta} \left(\frac{\delta E}{T} \right)^2 T^2 \qquad (15)$$

for stress along either a $\langle 111 \rangle$ or $\langle 100 \rangle$ direction. Here δE is the linear shift of the V_1 band and Δ is the spin-orbit splitting; the ratio $\delta E/T$ is a function only of the deformation potentials and the elastic constants. Substitution of either our acceptor ground-state deformation potentials or Laude's[45] band-edge deformation potentials into (15) yields values of the quadratic coefficient which differ from our observed values by less than a factor of 2. Since the maximum stress used was only of the order of 3×10^9 dyn/cm^2 Laude's[45] parameters b

TABLE II. Quadratic coefficient of stress splitting in units of $meV/(dyn/cm^2)^2$.

Stress direction	Expt.	Calc. (band edge)	Calc. (impurity)
$\langle 111 \rangle$	$(1.51 \pm 0.08) \times 10^{-19}$	$(1.98 \pm 0.10) \times 10^{-19}$	$(1.01 \pm 0.04) \times 10^{-19}$
$\langle 100 \rangle$	$(1.58 \pm 0.10) \times 10^{-19}$	$(1.21 \pm 0.08) \times 10^{-19}$	$(0.86 \pm 0.05) \times 10^{-19}$

and d and not b' and d' were used in calculating the quadratic shift. The experimental and calculated values of the quadratic coefficients are given in Table II.

The discrepancy between calculated and observed values is not too surprising since the theory for the valence-band edge leading to Eq. (15) cannot be taken over and directly applied to the acceptor ground state. However, one might expect that for sufficiently high stress the high-energy Raman component would have the same stress dependence as the V_1 valance-band edge. This is because the warping of the valence band disappears in the high-stress region.

The quadratic shift of the Raman component does not necessarily result solely from a quadratic shift of the acceptor ground state but may very well include a contribution from the excited state. If the excited state is associated with the spin-orbit split-off band, it should have a quadratic shift of opposite sign to that of the V_1 valence-band edge. This shift would result in an increased value of the Raman shift. With our experiment, however, it is impossible to distinguish between ground- and excited-state shifts. An effect that could be interpreted as a quadratic shift was also observed in the infrared absorption measurements of Chandrasekhar et al. [43] but it was not analyzed quantitatively.

The relative intensity of the two stress-split Raman components depends on the temperature of the sample according to the Boltzmann factor. Symmetry effects analogous to those discussed by Kaplyanskii [46] and by Rodriguez et al. [47] for infrared absorption under stress appear to be negligible here because temperature measurements based on the simple Boltzmann relation showed no systematic variation with stress. The sample temperature for these measurements was estimated at (16 ± 3) °K.

B. Acceptor g-Value Measurements

Figure 4 shows the electronic Raman line in boron-doped silicon under three sets of experimental conditions. The top trace is the zero-field spectrum; the other two traces show the Zeeman spectra at two different temperatures. The trace labeled "immersed" was taken with the sample immersed in liquid helium pumped below the λ point while the other two traces were taken with the sample mounted on a helium cold finger. Figure 5

demonstrates the anisotropy of the Zeeman splittings. The solid curves are experimental spectra; all of these spectra were taken with the sample mounted on the helium cold finger, and represent the average of scans. The dashed curves are the computed spectra using a method explained below.

Standard group-theoretical analysis shows that all eight of the possible Zeeman components of a Raman transition from a fourfold degenerate Γ_8 level to a twofold Γ_6 or Γ_7 level are allowed for unpolarized radiation. (This result is analogous to that of Lin-Chung and Wallis [48] who considered Raman transitions from a Γ_8 level to a Γ_8 level.) The experimental results, however, indicate that we have resolved only the Zeeman splitting of the acceptor ground state. In all three of the experimental spectra of Fig. 5 the component with the largest Raman shift has the largest intensity. A comparison of the two Zeeman spectra in Fig. 4 shows that this strong component gets even stronger at very low temperatures while the two components with the smallest Raman shifts practically disappear. This thermalizing behavior of the $\langle 111 \rangle$ spectra indicates that the four Zeeman components
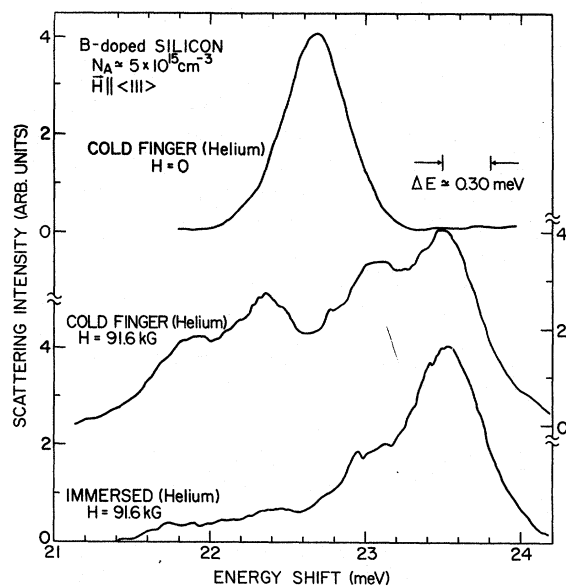
FIG. 4. Temperature dependence of Zeeman splitting of electronic Raman scattering in boron-doped silicon with magnetic field $\vec{H}$ applied along a $\langle 111 \rangle$ axis.
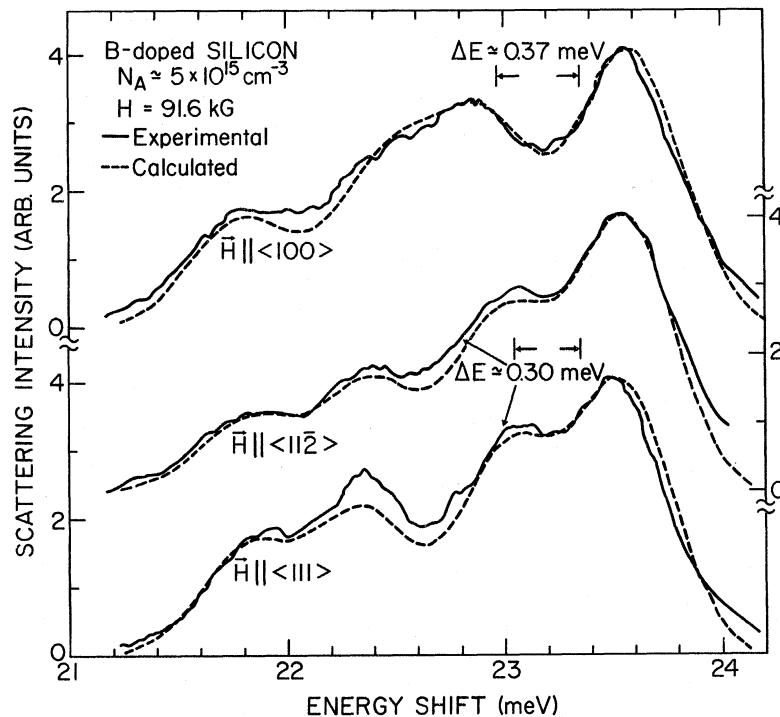
FIG. 5. Anisotropy of Zeeman splitting of electronic Raman scattering in boron-doped silicon with the sample mounted on a helium cold finger.

arise only from the fourfold splitting of the acceptor ground state, and that the splitting of the excited state is not large enough to be resolved. The relative intensities of the four Zeeman components are then a result of a Boltzmann population distribution similar to that described in the previous section.

With this interpretation the anisotropy seen in Fig. 4 is just that of the acceptor ground state. Using M^2 and ϵ as two adjustable parameters we calculated sets of self-consistent ground-state g values for magnetic fields along $\langle 100 \rangle$, $\langle 11\bar{2} \rangle$, and $\langle 111 \rangle$ directions. We then programmed a computer to generate the spectra which were predicted by these g values under the assumption of no excited-state splitting. Each calculated spectrum was the superposition of four Gaussian curves, one for each of the ground-state sublevels. The relative amplitude of each Gaussian was given by a Boltzmann factor and the width of each of them was set equal to the zero-field linewidth. The sample temperatures were estimated at 22 °K and were varied slightly in order to fit the experimental data better. The dashed curves in Fig. 5 are the best self-consistent fit to the experimental results. The self-consistent set of parameters is given in Table III.

Although we could not obtain a numerical value for the excited-state g factor g_{ex}, we set an upper limit for it by studying the line-broadening effects of nonzero g_{ex} by a computer simulation similar to that described above. In this way, we estimate

$g_{ex} \lesssim 0.4$. Using Eqs. (9) and (10) we can evaluate the parameters K and L in the spin Hamiltonian of Eq. (3) as $K = 0.84 \pm 0.09$, and $L = 0.13 \pm 0.08$. The errors associated with K and L are somewhat misleading because the errors in K and L are not independent.

These values of K and L are in fair agreement with the theoretical predictions of Suzuki et al.[25] in Eq. (4). Because of the inherent inaccuracies of the theory this agreement is probably as good as could have been hoped for. However, our experimental values are in significant disagreement with the results of Feher et al.[14] obtained by paramagnetic resonance under stress. Their results for the boron acceptor ground state were $g_{\parallel} = 1.21 \pm 0.01$, and $g_{\perp} = 2.43 \pm 0.01$. In these measurements uniaxial stress was applied along a $\langle 100 \rangle$ direction and a magnetic field applied parallel or perpendicular to the stress axis. Under the assumption of complete stress decoupling of the valence band $g_{\parallel}$ and $g_{\perp}$ are related to the spin Hamiltonian parameters by

$$g_{\parallel} = K + \tfrac{1}{4}L, \qquad g_{\perp} = 2K + 5L. \tag{16}$$

TABLE III. Boron acceptor ground-state g values.

$M^2 = 1.23 \pm 0.04$,	$\epsilon = -0.07 \pm 0.02$	
$\langle 100 \rangle$	$\langle 112 \rangle$	$\langle 111 \rangle$
g_i	0.88 ± 0.06	1.18 ± 0.03	1.26 ± 0.04
g_0	1.13 ± 0.03	1.11 ± 0.01	1.10 ± 0.02
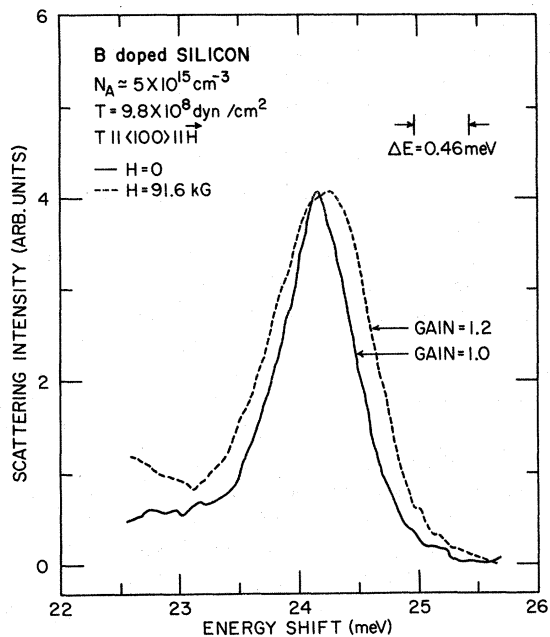
FIG. 6. Electronic Raman scattering in boron-doped silicon under simultaneous application of stress T and magnetic field $\vec{H}$. The solid curve gives the $H = 0$ spectrum and the dashed curve gives the spectrum for $H = 91.6$ kG.

The results of Feher *et al.*[14] then yield $K = 1.21 \pm 0.01$ and $L = 0.00 \pm 0.01$. The anisotropy which we observed appears qualitatively different from the isotropic situation predicted by these parameters. Feher *et al.*[14] noted that their results differed only slightly for stresses applied along other axes.

In order to investigate the discrepancy between the two sets of experimental results and to look for any stress dependence of the g value we have carried out magneto-Raman measurements on a stressed sample. A stress of 9.8×10^8 dyn/cm^2 applied along a $\langle 100 \rangle$ direction split the impurity Raman line into two components as discussed previously. However, the intensity of the component with the smaller Raman shift was negligible because of thermalizing effects. The observable component which is the one associated with the V_1 valence band is shown by the solid curve in Fig. 6. The dashed line in the figure represents this component observed with a magnetic field of 91.6 kG applied parallel to the stress axis. The Raman line is broadened by the magnetic field but no Zeeman components are resolved. The small bump on the low-energy side of the magnetic-field-broadened line results from the Zeeman splitting of the Raman component associated with the $M_j = \pm \frac{3}{2}$ valence band (V_2). The Zeeman splitting reduces the energy of one of these levels enough so as to repopulate it.

Even though no Zeeman components were resolved in this case, $g_{\parallel}$ for the acceptor ground state was estimated by a computer curve-fitting procedure similar to that described above. The best fit to the data was obtained with $g_{\parallel} = 0.9$. This is illustrated in Fig. 7(a). The solid curve is the experimental spectrum and the dashed curve is the calculated one. In Fig. 7(b) calculated spectra with values
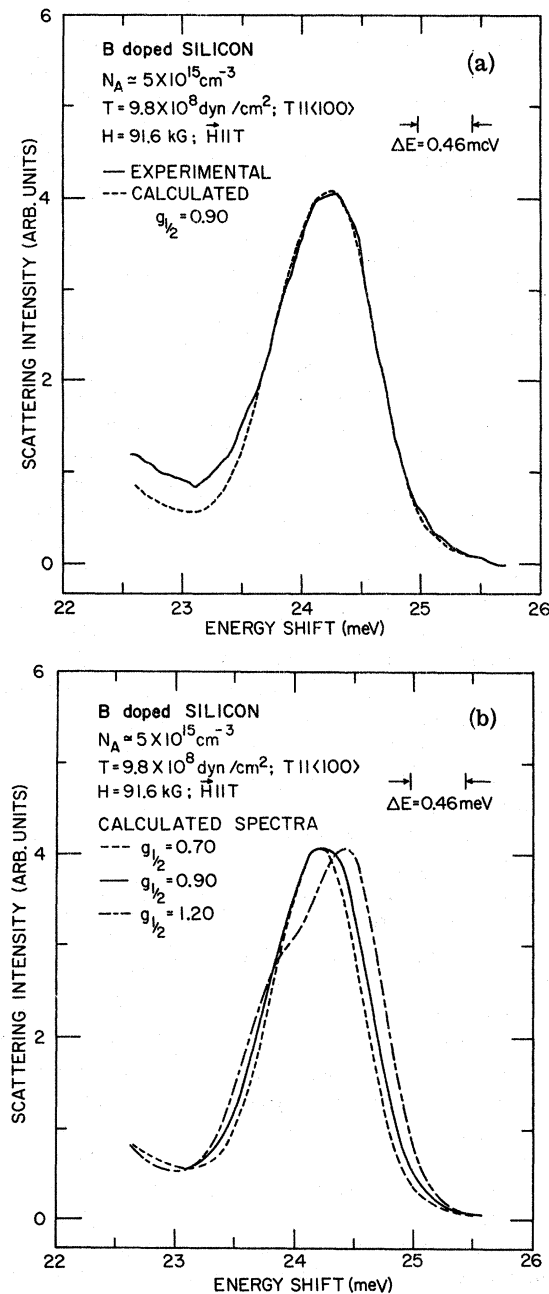
FIG. 7. Electronic Raman scattering in boron-doped silicon with $T \parallel \vec{H} \parallel \langle 100 \rangle$: (a) comparison of observed spectrum (solid curve) with a calculated spectrum (dashed curve) using $g_{1/2} = 0.9$; (b) calculated spectra for three different values of $g_{1/2}$.

of $g_{\parallel}$ of 0.7, 0.9, and 1.2 are shown. These curves demonstrate that our line-shape analysis is sufficiently sensitive to make a determination of the g value, and an estimate of the error. We have then for this case $g_{\parallel} = g_{1/2} = 0.9 \pm 0.1$. This value of $g_{1/2}$ agrees with the magneto-Raman result obtained at zero stress and differs from that of Feher et al.[14] The sensitivity of the curve-fitting procedure is sufficient for the discrepancy to be considered significant. However, the stress dependence of the g value $\Delta g_{\perp}/T = 7 \times 10^{-11}$ cm^2/dyn reported by Feher et al.[14] is too small to be measured in the present experiment. These observations rule out a stress dependence of the g value as an explanation for the discrepancy between the microwave resonance results and the magneto-Raman results.

The calculated values for the spin Hamiltonian predict an anisotropy qualitatively similar to that observed in the present experiment. However, the inadequacies of the calculation preclude more than a qualitative comparison.

The strength of the magnetic field used in the magneto-Raman experiment was about 90 kG while that used in the paramagnetic resonance experiment was about 3 kG. However, no magnetic field dependence of the g value is anticipated, because, even with a field of 90 kG, the magnetic energy of the bound hole, $g\mu_B H$, is very much less than all other relevant energies. Unfortunately, because of the poor resolution of the magneto-Raman experiments it was impossible to measure all the g values for a range of magnetic fields. However, $g_{3/2}(\langle 111 \rangle)$ was measured with the immersion Dewar for fields between 50 and 90 kG; all of these measurements were in agreement with the value given in Table III.

If the anisotropic term L in the spin Hamiltonian were introduced only by the vibronic coupling, then it would be expected to decrease with the application of stress; that is, the stress decoupling of the band partially turns off the vibronic interaction. Thus, the present experimental results indicate that the vibronic coupling is not the primary cause of the anisotropy in the ground-state g value. This is consistent with the results of a recent magneto-thermal conductivity experiment in p-type silicon[49] which indicated that vibronic coupling effects are small.

However, a possible explanation for the small g value of the excited state is that the vibronic coupling quenches the g value by mixing together the $M_j = \pm \frac{1}{2}$ states. Manchon and Dean[11] have discussed possible mechanisms for the coupling to the lattice of the analogous excited state in gallium phosphide.

Another possible explanation for the small observed g value is the existence of additional selec-

tion rules which reduce the number of allowed Raman transition between the sublevels from eight to four. There is, however, no theoretical basis for any such selection rules.

C. Bound-Exciton Photoluminescence

Arsenic donors were chosen for study because the photoluminescence from bound excitons is stronger for this donor than for any other. Also, the ratio of the intensity of the no-phonon recombination radiation to that of the TO-phonon-assisted recombination radiation is higher for this donor. This consideration is significant because of the large falloff in the sensitivity of an S-1 photomultiplier between the no-phonon line at 1.1492 eV and the TO-assisted line at 1.0911 eV.

Figure 8 illustrates the Zeeman splitting of the bound-exciton no-phonon photoluminescence in arsenic-doped silicon for various magnetic field directions and also includes a zero-field spectrum. The solid curves are experimental spectra and the dashed curves are calculated spectra obtained by a method similar to that used for the Raman scattering experiments described above. The fitting procedure will be discussed again below. All of the spectra in this figure were taken with the sample mounted in the cold-finger Dewar.
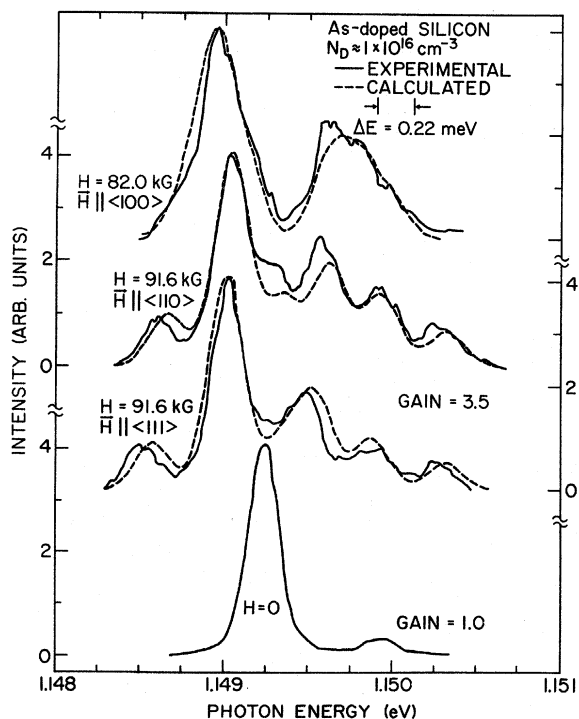
FIG. 8. Anisotropy of Zeeman splitting of photoluminescence from excitons bound to neutral donors in arsenic-doped silicon with the sample mounted on a helium cold finger. The solid curves give the observed spectra, and the dashed curves represent the computed spectra.
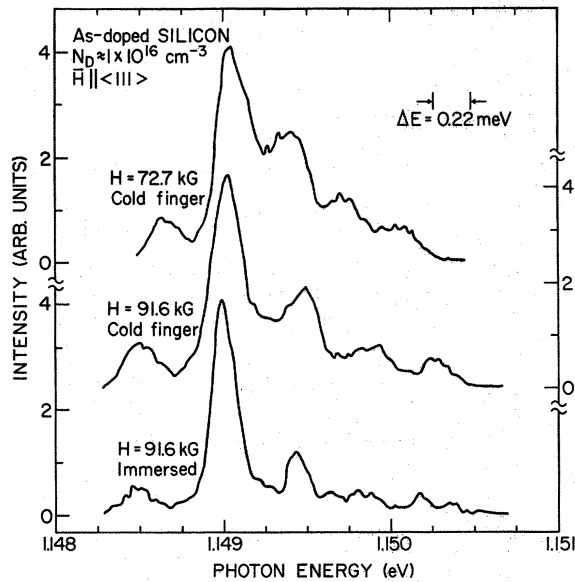
FIG. 9. Thermalization behavior of Zeeman splitting from excitons bound to neutral arsenic donors in silicon.

This figure shows the marked anisotropy of the Zeeman pattern and also indicates that the center of the Zeeman pattern is higher in energy than the zero-field line.

Figure 9 shows the thermalizing effects on the Zeeman splitting due to variations in the sample temperature and in the magnitude of the applied magnetic field. The bottom trace was taken with the sample immersed in liquid helium pumped below the λ point.

Figure 10 shows the polarization properties of the Zeeman pattern. Both spectra were taken with the sample mounted in the cold-finger Dewar and with HR sheet Polaroid used as a polarizer. The difference in gain of the two traces reflects the polarization dependence of the spectrometer throughout.

The width of the zero-field spectrum in Fig. 8 results from instrumental broadening. Additional measurements of the linewidth taken with narrower spectrometer slits have shown that the full width at half-maximum of the line is ≤ 0.1 meV in contrast to the value of ≤ 0.5 meV obtained by Haynes.[6] The improvement in the linewidth arises from the use of laser excitation rather than mercury lamp excitation. Any real width of the line is probably due to thermal or stress broadening. The samples used in this experiment and also in the study by Pokrovskii et al.[41] were more lightly doped than those used by Haynes and co-workers.[6,7]

Since the optical system favored the perpendicular polarization by a factor of 2.2, Fig. 10 indicates that the lines labeled 4 and 5 are partially polarized parallel to the magnetic field and the

lines labeled 2, 3, 6, and 7 are essentially unpolarized. This observation differs from the theoretical predictions. Although we do not have an explanation for the discrepancy, we have identified the four unpolarized components as corresponding to the four components predicted for $\vec{E} \perp \vec{H}$.

The peak labeled 6 in the $\langle 110 \rangle$ spectrum in Fig. 10 and the corresponding peak in the $\langle 111 \rangle$ spectrum are the largest peaks in their respective spectra. (Component 5 in the $\langle 110 \rangle$ spectrum is the one which does not correspond to any line in the $\langle 111 \rangle$ spectrum.) The thermalization data in Fig. 9 indicate that the intensity of this peak relative to all of the others increases with an increase in the ratio H/T. Hence, this Zeeman component originates in the lowest-energy magnetic sublevel of the bound-exciton complex. Using this observation, the dipole selection rules, and the assumption that the electronic g value $g_e \approx 2.0$, we conclude that the numbering of the components in Fig. 10 corresponds with that in Fig. 1.

The electronic g value and the hole g values were calculated by a two step procedure. The fan chart in Fig. 11 shows the experimental position of the six peaks as a function of magnetic field strength for a field along a $\langle 112 \rangle$ direction, which is equivalent to a $\langle 110 \rangle$ direction according to Eqs. (5) and (6). The solid curves are a least-squares computer fit to the data. The displacement of each peak from the zero-field position was assumed to result from the superposition of the linear splitting and a phenomenological quadratic diamagnetic shift of the whole pattern. One quadratic and three linear parameters were used for the fitting. The linear terms then yielded the following g values:

$$g_e = 1.85 \pm 0.03, \quad g_{1/2} = 1.26 \pm 0.05, \quad g_{3/2} = 1.17 \pm 0.02,$$
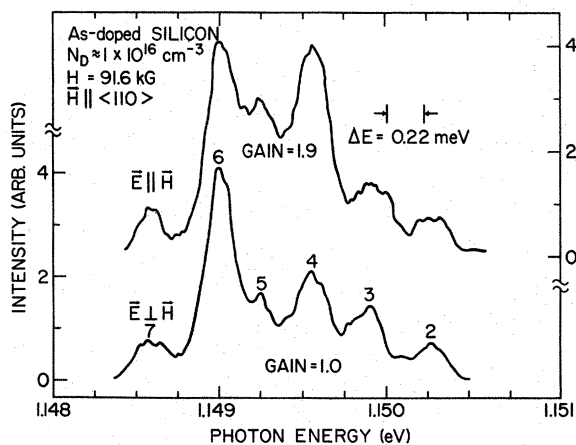
FIG. 10. Zeeman splitting of photoluminescence from excitons bound to neutral arsenic donors in silicon observed with a polarizer oriented either parallel or perpendicular to the applied magnetic field.
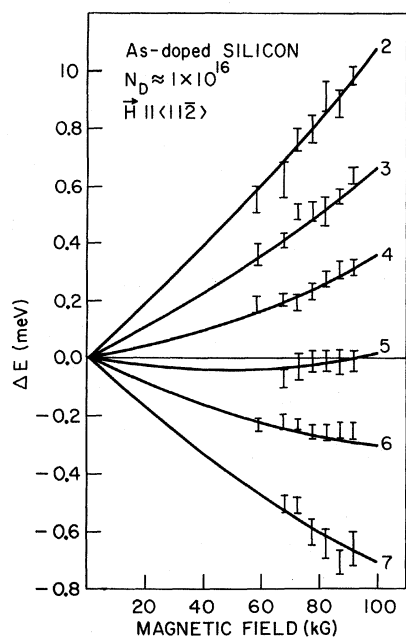
FIG. 11. Energy shifts as a function of magnetic field for Zeeman components of photoluminescence from excitons bound to neutral arsenic donors in silicon.

while the phenomenological quadratic term was $(1.85 \pm 0.08) \times 10^{-5}$ meV/kG^2.

These g values were then taken as a first approximation in a calculation of a set of parameters which could fit the data obtained for various orientations of the magnetic field. This procedure, which eventually yielded the dashed curves in Fig. 8, was basically the same as that discussed before. However, the splitting of two states had to be considered and the amplitudes of the components were determined not only by the Boltzmann factors but also by the transition probabilities. No allowance was made for the polarization dependence of the system response because the amplitude of the parallel components appeared anomalously large. The quadratic shift was ignored in the calculation. In the preparation of Fig. 8 the computed spectra were simply displaced in energy so that they were in coincidence with the experimental spectra at the position of the highest peak. They were normalized so that the amplitude of the highest peaks would be the same in all the traces. The temperature used for fitting these curves was 20 °K.

The final values for the phenomenological parameters of Yafet and Thomas for the hole g value were $M^2 = 1.44 \pm 0.07$ and $\epsilon = -0.12 \pm 0.04$, and for the electron g value, $g_e = 1.85 \pm 0.06$. The estimated errors are somewhat arbitrary; they correspond to the limits of values of the parameters which give over-all reasonable fits to the data. The parameters used for the calculated spectra in

Fig. 8 are listed in Table IV; they all correspond to $M^2 = 1.44$ and $\epsilon = -0.12$. The corresponding spin Hamiltonian parameters are $K = 0.74$, and $L = 0.22$. No errors are attached to these parameters because the errors are not independent.

The g value of the donor ground state was also obtained in a more direct way in order to avoid uncertainties resulting from the quadratic shift. The hypothesis of a single quadratic coefficient for all of the Zeeman components is arbitrary and appears not to be completely accurate. However, from Fig. 1 it is seen that g_e is given directly by the energy difference between components 4 and 7. In Fig. 12 this energy difference is plotted as a function of magnetic field. The solid line drawn corresponding to $g_e = 1.85$ gives a reasonable fit to the data while the dashed line drawn for $g_e = 2.00$ gives a poor fit.

The g value of the arsenic donor ground state had been previously measured very precisely by Feher[21] using electron nuclear double resonance as $g_e = 1.99867 \pm 0.00010$. Figure 12 shows that this value is inconsistent with our measurements. Additional data taken with a magnetic field along a $\langle 111 \rangle$ direction are consistent with the low g value; none are consistent with $g_e = 2.00$. This discrepancy appears significant and may indicate that the Thomas model is somewhat oversimplified. In previous optical studies of the Zeeman splitting of radiative recombination from excitons bound to neutral donors in gallium phosphide[19,20] and in cubic silicon carbide[50] the measured value of g_e using the Thomas model was less than that obtained in microwave resonance experiments.[51,52] Also, there is a similar relation between magneto-optical[52] and resonance[53] values of the g factor for the tin donor in gallium phosphide. Tin is a gallium site donor and therefore the Thomas model does not apply directly. All of these experimental results are listed in Table V. The errors in these other optical measurements overlap the resonance results; however, there may be some significance in the fact that optical measurements gave lower g values in all these different materials.

We have attributed the diamagnetic shift of the Zeeman pattern in Fig. 8 to a quadratic diamagnetic Zeeman effect for the bound exciton. This is the first observation of such an effect for excitons bound to neutral donors; however, its

TABLE IV. g values used for calculated spectra in Fig. 8.

Direction of $\vec{H}$	g_e	$g_{1/2}$	$g_{3/2}$
$\langle 111 \rangle$	1.85	1.46	1.17
$\langle 110 \rangle$	1.85	1.31	1.19
$\langle 100 \rangle$	1.85	0.79	1.24
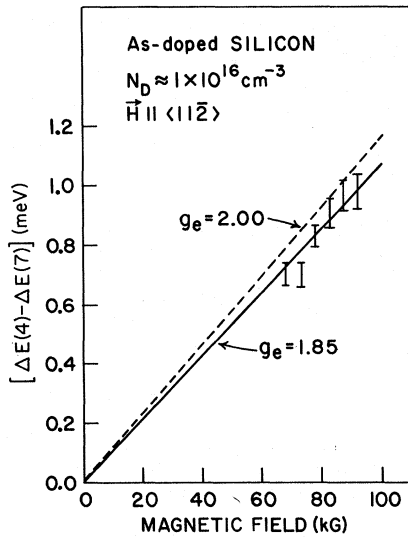
FIG. 12. Determination of electron g values g_e from Zeeman splitting of photoluminescence from excitons bound to neutral arsenic donors in silicon. The solid line is for $g_e = 1.85$ and the dotted line is for $g_e = 2.00$.

existence is hardly surprising. In any Hamiltonian containing the vector potential as $(\vec{p} - e\vec{A}/c)^2$ there is a term in A^2 which becomes observable for sufficiently intense magnetic fields. Our data are not sufficiently accurate to confirm that the diamagnetic shift is really a quadratic effect, but this type of shift appears to be the most plausible explanation.

Zwerdling et al.[54] have reported a quadratic shift of the free indirect exciton in germanium, whose magnitude was in rough agreement with that expected from a hydrogenic atom. Using a similar approximation for the reduced mass we have calculated the expected diamagnetic shift of the indirect free exciton in silicon. This value differs from our measured quadratic shift by less than a factor of 3.

The small bump at 1.1499 eV seen in the zero-field trace in Fig. 8 was not reported previously. This feature, however, was reproducible and was observed in spectra taken with all of the samples used. A similar feature was also observed on the high-energy side of the TO-phonon-assisted transition. It is possible that this feature represents an excited state of the bound-exciton complex; since it is on the high-energy side of the no-phonon transition it cannot have any connection with the donor electron. The observation of the feature in spectra taken with the sample immersed in liquid helium, however, argues against this interpretation because

TABLE V. Comparison of optical and microwave determination of g values of ground state of donor electrons.

Material (donor)	Optical	Microwave
Si (As)	1.85 ± 0.06[a]	1.99867 ± 0.00010[b]
GaP (S)	1.89 ± 0.10[c]	1.9976 ± 0.0008[d]
GaP (Sn)	1.95 ± 0.06[e]	1.995 ± 0.002[f]
Cubic SiC (point defect)	1.96 ± 0.06[b]	2.00445 ± 0.0001[g]

[a]This work
[b]Reference 21.
[c]Reference 20.
[d]Reference 51.
[e]Reference 52.
[f]Reference 53.
[g]Reference 50.

of expected thermalizing effects. The intensity of this unidentified feature was sufficiently small that it was ignored in the analysis of the Zeeman splitting.

V. CONCLUSION

The magneto- and piezo-Raman measurements reported here have yielded the g value and deformation potentials for the ground state of the boron acceptor in silicon. The deformation potentials are in good agreement with other measurements; however, the g values obtained are inconsistent with the results of paramagnetic resonance experiments. The inconsistency has not been resolved. The anomalously small g value deduced for the excited state in the Raman transition indicates the need for additional theoretical calculations as to the nature of this state.

The observed Zeeman splitting of the photoluminescence from excitons bound to neutral donors in arsenic-doped silicon is in good agreement with the model of Thomas et al. However, the measured g value of the ground state of the arsenic donor is in disagreement with spin resonance results.

*Also, Physics Department, Massachusetts Institute of Technology, Cambridge, Mass. 02139.

†Present address: Departments of Physics and Electrical Engineering, University of Southern California, Los Angeles,

Calif. 90007.

†Supported by the National Science Foundation.

[1]For donors, see R. L. Aggarwal and A. K. Ramdas, Phys. Rev. 137, A602 (1965).

[2]For acceptors, see A. Onton, P. Fisher, and A. K. Ramdas, Phys. Rev. 163, 686 (1967).

[3]G. B. Wright and A. Mooradian, Phys. Rev. Lett. 18, 608 (1967).

[4]G. B. Wright and A. Mooradian, Bull. Am. Phys. Soc. 13, 47 (1966).

[5]G. B. Wright and A. Mooradian, in Proceedings of the Ninth International Conference on the Physics of Semiconductors, Moscow, 1968 (Nauka, Leningrad, 1969), p. 1067.

[6]J. R. Haynes, Phys. Rev. Lett. 4, 361 (1960).

[7]P. J. Dean, J. R. Haynes, and W. F. Flood, Phys. Rev. 161, 711 (1967).

[8]P. J. Dean, W. F. Flood, and G. Kaminsky, Phys. Rev. 163, 721 (1967).

[9]D. F. Nelson, J. D. Cuthbert, P. J. Dean, and D. G. Thomas, Phys. Rev. Lett. 17, 1262 (1966).

[10]C. H. Henry, J. J. Hopfield, and L. C. Luther, Phys. Rev. Lett. 17, 1178 (1966).

[11]D. D. Manchon, Jr. and P. J. Dean, in Proceedings of the Tenth International Conference on the Physics of Semiconductors, Cambridge, Mass., 1970, edited by S. P. Keller, J. C. Hensel, and F. Stern (U.S. AEC Div. Tech. Info., Springfield, Va., 1970), p. 760.

[12]T. N. Morgan, Phys. Rev. Lett. 24, 887 (1970).

[13]S. Zwerdling, K. J. Button, and B. Lax, Phys. Rev. 118, 975 (1960).

[14]G. Feher, J. C. Hensel, and E. A. Gere, Phys. Rev. Lett. 5, 309 (1960).

[15]J. M. Cherlow, R. L. Aggarwal, and B. Lax, Bull. Am. Phys. Soc. 17, 258 (1972).

[16]J. M. Cherlow, R. L. Aggarwal, R. Ranvaud, and B. Lax, in Proceedings of the Eleventh International Conference on the

Physics of Semiconductiors, Warsaw, 1972 (PWN-Polish Scientific Publishers, Warszawa, 1972), p. 1154.

[17]M. A. Lampert, Phys. Rev. Lett. 1, 450 (1958).

[18]J. M. Cherlow, R. L. Aggarwal, and B. Lax, Bull. Am. Phys. Soc. 16, 328 (1971).

[19]D. G. Thomas, M. Gershenzon, and J. J. Hopfield, Phys. Rev. 131, 2397 (1963).

[20]Y. Yafet and D. G. Thomas, Phys. Rev. 131, 2405 (1963).

[21]G. Feher, Phys. Rev. 114, 1219 (1959).

[22]S. Zwerdling, K. J. Button, B. Lax, and L. M. Roth, Phys. Rev. Lett. 4, 173 (1960).

[23]J. M. Luttinger and W. Kohn, Phys. Rev. 97, 869 (1955).

[24]D. Schechter, Ph.D. thesis (Carnegie Institute of Technology, 1958) (unpublished); J. Phys. Chem. Solids 23, 237 (1962).

[25]K. Suzuki, M. Okazaki, and H. Hasegawa, J. Phys. Soc. Jap. 19, 930 (1964).

[26]G. E. Pikus and G. L. Bir, Fiz. Tverd. Tela 1, 1642 (1959) [Sov. Phys.-Solid State 1, 1502 (1960)].

[27]W. H. Kleiner and L. M. Roth, Phys. Rev. Lett. 2, 334 (1959).

[28]J. M. Luttinger, Phys. Rev. 102, 1030 (1956).

[29]H. Hasegawa, Phys. Rev. 129, 1029 (1963).

[30]J. C. Hensel and G. Feher, Phys. Rev. 129, 1041 (1963).

[31]B. Bleaney, Proc. Phys. Soc. Lond. 73, 939 (1959).

[32]A. K. Bhattacharjee and S. Rodriguez, Phys. Rev. B 6, 3836 (1972).

[33]I. Balslev and P. Lawaetz, Phys. Lett. 19, 6 (1965).

[34]G. L. Bir, E. I. Butikov, and G. E. Pikus, J. Phys. Chem. Solids 24, 1467 (1963).

[35]T. N. Morgan, in Ref. 11, p. 266.

[36]J. C. Phillips, Phys. Rev. B 2, 4044 (1970).

[37]J. J. Hopfield, in Proceedings of the International Conference on the Physics of Semiconductors, Paris, 1964 (Dunod Cie, Paris, 1964), p. 725.

Boron, the Dominant Acceptor in Semiconducting Diamond

R. M. Chrenko

General Electric, Corporate Research and Development, Schenectady, New York 12301

(Received 6 November 1972)

A study has been made to determine the nature of the acceptor center in laboratory-grown semiconducting diamonds. Analyses for nitrogen, aluminum, boron, and uncompensated-acceptor content of aluminum and boron-doped crystals have shown that (i) the aluminum content of inclusion-free crystals is very low, (ii) there is not enough aluminum to account for the acceptor content, (iii) the nitrogen content is very low and only a small degree of compensation by deep-lying nitrogen donors could exist for many semiconducting diamonds, and (iv) there is a good correlation between boron content and acceptor content. These results indicate that boron is the dominant acceptor in laboratory-grown semiconducting diamond, and not aluminum as has been assumed previously by a number of authors. These results, when combined with other data on resistivity and activation energy for conduction, indicate that the dominant semiconducting properties of both natural and laboratory-grown diamond are due to one acceptor, boron, at different concentrations. Previous papers on laboratory-grown semiconducting diamonds which based arguments on the large aluminum content and the assumed high nitrogen content are critically reexamined.

I. INTRODUCTION

The purpose of this study was to determine the nature of the acceptor center in semiconducting diamond. The qualitative and quantitative results presented here indicate that the dominant acceptor is boron, and not aluminum, as has been assumed previously by a number of authors.

Semiconducting, or type-IIb,[1] diamonds, were first recognized by Custers.[2,3] A number of papers have been published subsequently on their electrical and optical properties. The activation